Revisiting the Stimulation-Rate-Dependent Pattern Mismatch Negativity

Marc Pabst

Affiliation

Course Title

Professor Name

Due Date

Abstract

How does the brain process and represent successive sound in close temporal proximity? By investigating mismatch negativity (MMN) components, prior research (Sussman & Gumenyuk, 2005; Sussman, Ritter & Vaughan, 1998) has suggested that temporal proximity plays an important role in how sounds are represented in auditory memory. Here, we investigate how predictability affects the election of mismatch negativity components in auditory sequences consisting of two tones (frequent tone A = 440 Hz, rare tone B = 494 Hz, fixed SOA 100 ms). In the predictable condition, tones are presented in a fixed order whereas in the unpredictable condition, standards and deviants are presented in a pseudo-random order. We expect to find that B tones in the unpredictable condition will elicit a significant MMN while B tones in the predictable conditions will not. A repeating five-tone pattern was presented at several stimulus rates (200, 400, 600, and 00 ms onset-to-onset) to determine at what temporal proximity the five-tone repeating unit would be represented in memory. The mismatch negativity component of event-related brain potentials was used to index how the sounds were organized in memory when participants had no task with the sounds. Only at the 200-ms onset-to-onset pace was the five-tone sequence unitized in memory. At presentation rates of 400 ms and above, the regularity (a different frequency tone occurred every fifth tone) was not detected and mismatch negativity was elicited by these tones in the sequence. The results show that temporal proximity plays a role in unitizing successive sounds in auditory memory. These results also suggest that global relationships between successive sounds are represented at the level of auditory cortices.

Revisiting the Stimulation-Rate-Dependent Pattern Mismatch Negativity

Introduction

– Introducing oddball paradigm – The auditory oddball paradigm is a well-established type of experimental design extensivly used in event related potential (ERP) studies. In its basic form, subjects are presented with a series of similar tones or sounds (so-called *standards*), interrupted by rare tones or sounds that differ in at least one feature (*deviants*) from the more frequent ones. Since it is assumed that the brain constantly makes predictions about future sensory impressions and deviating auditory events must violate these predictions, these rare sounds play an important role in understanding prediction and expectation in the human brain. Different measures have been used to quantify differenced in processing between *standard* and *deviant* events,

– introducing MMN – One of the best-studied approaches to measure these differences in processing is known as the missmatch negativity (MMN) component, obtained by subtracting the reponse to deviant events from the resposne to standard events. Negativity is strongest in the fronto-temporal area of the scalp with a peak latency ranging from 100 to 250 ms after stimulus onset. The eliction of MMN is not restricted to the reptition of physically identical stimuli but can also be observed when deviant events are of complex nature, e.g. when abstract auditory regularities are violated (**???**). The regularities can come in the form of relationships between two Saarinen et al. (1992) or multiple tones (Alain et al., 1994; Nordby et al., 1988; Schröger et al., 1996) a

– introducing sussmans study – Sussman et al. (1998) presented participants with a sequency of frequent pure tones and rare pitch deviants. Tones were arranged in a predictable five-tone pattern consisting of four standard tones and one deviant (i.e. A-A-A-A-B-A-A-A-A-B, ''-'' indicating silence between the tones). ERPs to A and B tones were compared for rapid (SOA of 100 ms) and slow (SOA of 1200 ms) stimulation rates. For the 100 ms SOA, they also included a control condition in which tone order was pseudo-random (e.g. A-A-A-B-A-B-A-A-A) without altering deviant probability ($p_B = 20\%$). MMNs were only elicted if tone presentation was slow and predcitable or fast and random. In a subsquent study, Sussman & Gumenyuk (2005) used the same pattern at different SOAs (200 ms, 400 ms, and 800 ms). Simmilarly to their prevous study, grouped presentation at 400 ms and 800 ms SOA elicted a MMN, while at a stimulution rate of 200 ms such evidence was

absent. Sussman et al. attributed this observation to sensory memory limitations. Only when auditory memory accommodates enough repetitions of the five-tone pattern, tones could be integrated into a coherent representation allowing for accurate predictions of deviant tones (explaing the absence of MMNs. They further argued that while this must be the case for fast presentation rates with SOAs up to 200 ms, for longer SOAs pattern durations would be too long ans thus eceed sensory memory capacity. The main weakness in their study is that they ma

– scharf muller – In a recent in-class replication study, (**???**). found that simplified experimental setup

Methods and Materials

Data Acquisition

Participants

100 ms Presentation Rate Twenty-three psychology undergraduate students (2 males, average age 22.6 yrs., $SD = 5.57$, range 18 - 42 yrs.) were recruited at the Institute of Psychology at the University of Leipzig. All participants reported good general health, normal hearing and had normal or corrected-to-normal vision. Written informed consent was obtained before the experiment. One-third (34.8%) of participants spent time enaging in musical activities at time of survey, while 8.7% had no prior experience in music training. Handedness was asseced using a modified version of the Edinburgh Handedness Inventory (Oldfield, 1971, see appendix). A majoritiy (00%) of parcicipants favored the right hand. Particpants were blinded in respect to the purpose of the experiment and received course credit in compensation.

150 ms Presentation Rate Twenty healthy participants (0 males, average age 00.0 yrs., $SD = 0.00$, range 00 - 00 yrs.) were recruited. Particpants gave informed consent and reported normal hearing and corrected or corrected-to-normal vision. All participants were naive regarding the purpose of the experiment and were compensated in cource credit or money. 00 participants (00%) had received musical training in the last 5 years before the experiment while 00 (00%) reported no musical experiance. In addition, participants reported

if streaming occured during the presentation of the tones.

Stimuli and Stimulis Delivery

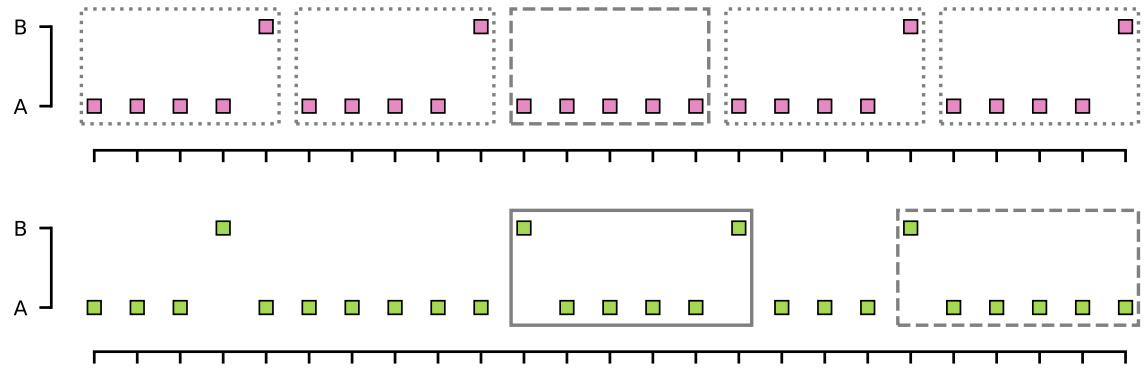

Figure 1. *Tones of two different frequencies (A=440 Hz, B=449 Hz) were presented in two blocked conditions: In the "predictable" condition (top half), tones followed a simple pattern in which a single B-tone followed four A-tones. Some designated B-tones were replaced by A-tones ("pattern deviants"). In the "random" condition (lower half), tones were presented in a pseudo-random fashion ()*

Participants where seated in a comfortable chair in a sound-insulated cabin. The experimental setup was practically the same as the one used ny Sussman, but instead of reading a book, subjects were asked to focus their attention on a previously selected movie. Movies were presented with subtitles but without sound. Commercially available software (MATLAB R2014a; The MathWorks Inc, Natick, MA) in conjunction with the Psychophysics Toolbox extension (version 3.0.12, Brainard, 1997; Kleiner et al., 2007) was used to control stimulus presentation. Stimuli consisted of pure sinusoidal tones with a duration of 50 ms (including a 10 ms cosine on/off ramp), presented isochronously at a stimulation onsets asynchrony (SOA) of 100 ms for study 1 and 150 ms for study 2. Overall, a total of 40 blocks containing a mixture of frequent 440 Hz tones ("A" tones) and infrequent 449 Hz tones ("B" tones) were delivered binaurally using Sennheiser XY headphones. In one half of the blocks, tones were presented in pseudo-random order (e.g. A-A-A-B-A-B-A}, "random" condition), while in the remaining block tone presentation followed a simple pattern in which a five-tone-sequence of four frequent tones and one infrequent tone (i.e. A-A-A-A-B) was repeated cyclically ("predictable" condition). The ratio of frequent and infrequent tones was 10% for both conditions. Within the predictable condition, 10% of designated (infrequent) B

tones were replaced by A tones, resulting in sporadic five-tone sequences consisting solely of A tones (i.e. A-A-A-A-A), thus violating the predictability rule. To assure comparability of local histories between tones in both conditions, randomly arranged tones were interspersed with sequences mimicking aforementioned patterns from the predictable condition (B-A-A-A-A-B and B-A-A-A-A-A) in the random condition. A grand total of 2000 tones in study 1 and 4000 tones in study 2 were delivered to each participant. The order of the runs was counterbalanced across participants.

Data Acquisition

Electrophysiological data was recorded from active silver-silver-chloride (*Ag-AgCl*) electrodes using an ActiveTwo amplifier system (BioSemi B.V., Amsterdam, The Netherlands). Acquisition was monitored online to ensure optimal data quality. A total of 39 channels were obtained using a 32-electrode-cap and 7 external electrodes. Scalp electrode locations conformed to the international 10–20 system. Horizontal and vertical eye movement was obtained using two bipolar configurations with electrodes placed around the lateral canthi of the eyes and above and below the right eye. Additionally, electrodes were placed on the tip of the nose and at the left and right mastoid sites. Data was sampled at 512 Hz and on-line filtered at 1000 Hz.

Analysis Pipeline

Data prepossessing was implemented using a custom pipeline based on the *MNE Python* software package (Gramfort, 2013) using *Python 3.7*. All computations were carried out on a cluster operated by the University Computation Center of the University of Leipzig. Code used in thesis is publicly available at https://github.com/marcpabst/xmas-oddballmatch.

First, EEG data was subjected to the ZapLine procedure (de Cheveigné, 2020) to remove line noise contamination. A fivefold detection procedure as described by Bigdely-Shamlo et al. (2015) was then used to detect and subsequently interpolate bad channels. This specifically included the detection of channels thain contain prolonged segments with verry small values (i.e. flat channels), the exclusion of channels based on robust standard deviation (deviation criterion), unusualy pronounced high-frequency noise (noisiness criterion), and the removal of channels that were poorly predicted by nearby channels

(correlation criterion and predictability criterion). Channels considered bad by one or more of these methods were removed and interpolated using spherical splines (Perrin et al., 1989). Electrode locations for interpolations were informed by the BESA Spherical Head Model.

For Independant Component Anaylsis (ICA), data 1-Hz-high-pass filtered (134th order hamming-windowed FIR) was applied prior to ICA (Winkler et al., 2015). To further reduce artifacts, Artifact Subspace Reconstruction (ASR, Mullen et al., 2015) was used to identify parts of the data with unusual characteristics (bursts) which were subsequently removed. ICA was then carried out using the *Picard* algorithm (Ablin et al., 2018, 2017) on PCA-whitened data. To avoid rank-deficiency when extracting components from data with one or more interpolated channels, PCA was also used for dimensionality reduction. The EEGLAB (version 2020.0, Delorme & Makeig, 2004) software package and the IClabel plugin (version 1.2.6, Pion-Tonachini et al., 2019) were used to automatically classify estimated components. Only components clearly classified (i.e. confidence above 50%) as resulting from either eye movement, muscular, or heartbeat activity were zeroed-out before applying the mixing matrix to unfiltered data.

In line with recommendations from Widmann et al. (2015) and de Cheveigné & Nelken (2019), a ORDER finite impulse response (FIR) bandpass filter from 0.1 Hz to 40 Hz (Hamming window, 0.1 Hz lower bandwith, 4 Hz upper bandwidth, 0.0194 passband ripple, and 53 dB stopband attenuation). Continuous data was epoched into 400 ms long segments around stimulus onsets. Epochs included a 100 ms pre-stimulus interval. No baseline correction was applied. Segments exeeding a peak-to-peak voltage difference of 100 µV were removed. No data set meet the pre-registrated exclusion criterion stated of less than 100 trials per condition, thus data from all participants (20 for 100 ms presentation rate and 23 for 150 ms presentation rate) was analysed.

Statistical Analysis

MMN

The dependent variable for analysing missmatch response was calculated by averaging amplitudes in a time window extedning ±25 ms around the maximum negativity obtained by subtracting the mean ERP timecourse following the (expected) deviant event from the ERP

following the (expected) standard event. To obtain mean amplitudes, ERPs to 4th position A tones (A-A-A-**A**-X, **boldface** indicates the tone of interest) and B tones (A-A-A-A-**B**) were averaged seperatly for both the *random* and the *predictable condition*. For the *random condition*, only tones that were part of a sequence matching the patterns in the *predictable* condition were included.

In accordance with the original analysis by Sussman & Gumenyuk (2005), mean amplitudes for frontocentral electrodes (FZ, F3, F4, FC1, and FC2) and the two mastoid positions (M1 and M2) were averaged separately. Then, for both SOAs, independant three-way repeated measures analyses of variance with factors *condition* (factors *predcitable* and *random*), *stimulus type* (factors *A tone* and *B tone*), *electrode locations* (levels *fronto-central* and *mastoids*), and all possible interactions were calculated.

It is commonly known that small SOAs []

Results

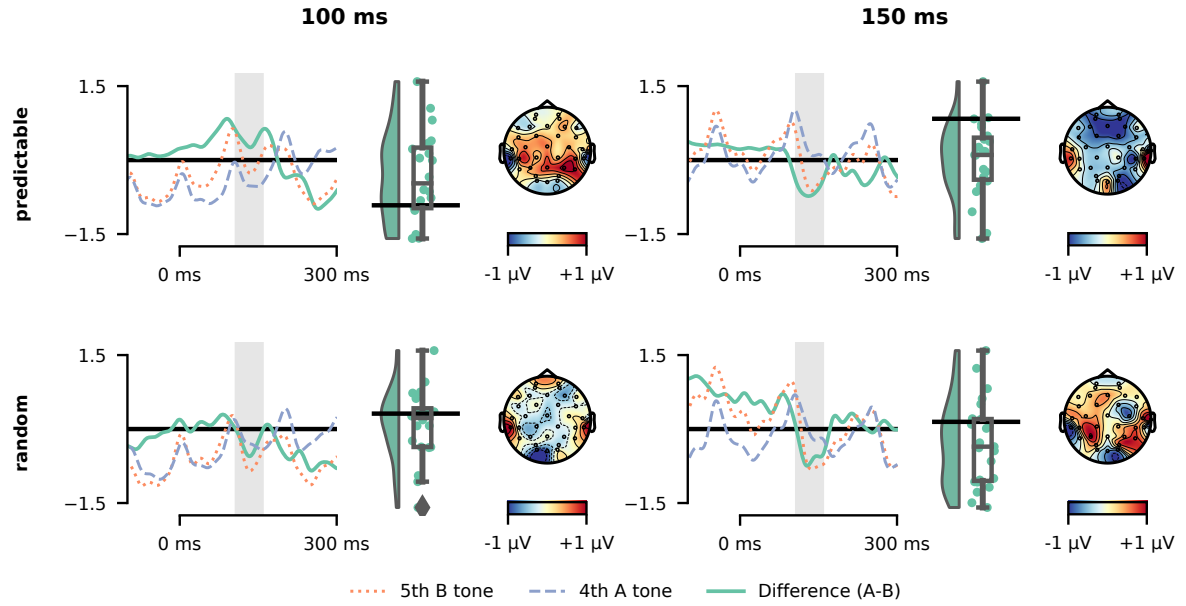

Figure 2. *ERP grand averages (pooled FZ, F3, F4, FC1, and FC2 electrode locations) for an SOA of 100 ms (left) and 150 ms (right), for A tones (A-A-A-**A**-X, blue dashed lines) and B tones (A-A-A-A-**B**, orange dashed line) and their difference (B - A, green solid line). Upper panels show ERPs for tones presented in a predcitable pattern (*predcitable condition*) while lower panels show ERPs for tones presented in pseudo-random order (*random condition*). Shaded area marks MMN latency window (110 ms to 160 ms) used to calculate the distribution of amplitude differences across particpants (middle of each panel) and the difference of topographic maps averaged over the same interval (right of each panel).*

Grand averages of event-related potentials (ERP) at pooled FZ, F3, F4, FC1, and FC2 electrode locations to A tones (A-A-A-**A**-X), B tones (A-A-A-A-**B**), and their difference (**B** tone minus **A** tone) are displayed in Figure X for both 100 ms (left panel) and 150 ms (right panel) stimulus onset asynchronies. Top half of each panel shows ERPs in the *predictable condition* while lower half depicts ERPs in the *random condition*. For both presentation rates, clear rythms matching the presentation frequency of 10 Hz (100 ms) and respectivly 6.667 Hz (150 ms) are seen as a result from substantial overlap of neighboring tones. Panels also show the distribution of mean amplitude differences in the MMN latency window (as defined above, 110 ms to 160 ms after stimulus onset) across particpants and the difference of sclap topogrphies averaged over the same interval. Simmilarly, waveforms and mean amplitude

difference distributions at pooled mastoid sites are shown in Figure X.

ERP grand averages (pooled M1, M2 electrode locations) for an SOA of 100 ms (left) and 150 ms (right), for A tones (A-A-A-**A**-X, blue dashed lines) and B tones (A-A-A-A-**B**, orange dashed line) and their difference (B - A, green solid line). Upper panels show ERPs for tones presented in a predcitable pattern (*predcitable condition*) while lower panels show ERPs for tones presented in pseudo-random order (*random condition*). Shaded area marks MMN latency window (110 ms to 160 ms) used to calculate the distribution of amplitude differences across particpants.

Evoked responses to A and B tones were compared by calculating mean amplitudes in the MMN latency window. Mean amplitudes in the MMN latency window and their standard deviantions (SD) for all conditions are shown in Table X. Descriptively, mean amplitudes at pooled fronto-central electrode locations were more negative for randomly presented B tones than for randomly presented A tones, regardless of tone presentation rate (100 ms: $\Delta M = -0.358\,\mu V$; 150 ms: $\Delta M = -0.555\,\mu V$) This also held true for tones presented in a predictable fashion, but for the slower of the two presentation rates only ($\Delta M = -0.582\,\mu V$)). In contrast, when predcitable tone patterns occured at a faster 100 ms rate, B tones elicted descriptively more positive responses than A tones ($\Delta M = 0.383\,\mu V$). Descriptive comparison of evoked responses from pooled left and right mostoids revealed that pseudo-randomly presented B tones were more positive in the MMN latency window than A tones (100-ms-SOA: $\Delta M = 0.746\,\mu V$, 150-ms-SOA: $\Delta M = 0.510\,\mu V$). A simmilar observation could be made for precitable B tones compared to the preceeding A tones at a SOA of 150 ms ($\Delta M = 0.399\,\mu V$)) but not for the faster presentation rate ($\Delta M = -0.132\,\mu V$).

Statistical analyses provided support for these findings. For the 100 ms stimulation rate, the three-way ANOVA yielded a significant three-way interaction effect (*condition* x *stimulus type* x *electrode locations*; $F(1, 19) = 7.53$, $p = 0.0130$) but failed to reveal main effects for factors *stimulus type* ($F(1, 19) = 1.05$, $p = 0.3180$), *condition* ($F(1, 19) = 0.83$, $p = 0.3730$), and *electrode locations* ($F(1, 19) = 0.04$, $p = 0.8520$). In contrast, for tones presented at a SOA of 150 ms only the two-way interaction term *stimulus type* x *electrode locations* had a significant effect ($F(1, 22) = 20.76$, $p = 0.0002$). Mean amplitudes in the MMN latency window however did not differ for factors *stimulus type* ($F(1, 22) = 0.32$, $p = 0.5790$),

SOA	Condition	StimulusType	Mean	SD	Mean	SD
100	predictable	A	-0.431	1.23	-0.052	1.51
		B	-0.0477	1.22	-0.184	1.56
	random	A	-0.225	1.82	-1.04	2.64
		B	-0.583	2.16	-0.296	3.23
150	predictable	A	0.25	0.967	-0.349	1.19
		B	-0.331	1.09	0.0492	1.33
	random	A	0.0233	1.75	-0.292	1.64
		B	-0.531	1.82	0.218	2.38

electrode locations ().

Two-way ANOVAs (*condition* x *stimulus type*) were carried out seperatly for pooled fronto-central and mostoid electrode locations. For 100 ms tone presenation rate, the *condition* x *stimulus type* interaction only revealed a significant effect for the fronto-central electrode cluster ($F(1, 19) = 16.75$, $p = 0.0006$) but not for pooled mastoid sites ($F(1, 19) = 2.37$, $p = 0.1410$) indicating that the three-way interaction effect condition x stimulus type x electrode is indeed driven by the amplitude differnces in te fronto-central electrode locations . Contrary to this, for the 150 ms presentation rate, main effects for *stimulus type* were significant for both fronto-central and mastoid sites, suggesting that there was both a MMN at fronto-central locations as well as a polarity-reversal at the mastoid electrodes.

Post-hoc tests between ERPs to A and B tones were carried out using paired Student's t-Tests. P-values were corrected for multiple comparisons using the Benjamini–Hochberg step-up procedure. For the 100 ms SOA, results indicate a significant effect only for predictable tones at fronto-central electrodes ($t(19) = -2.77$, $p = .025$, $d = -0.62$). For the 150 ms SOA, B tones elicted significantly more negative ERPs than B tones at fronto-central electrode locations in both the predictable ($t(22) = 5.20$, p< .001, $d = 1.08$) and random ($t(22) = 3.28$, $p = .009$, $d = 0.68$) conditions. Significant polarity reversal effects at mastoid sites was only present dor predcitable tones ($t(22) = -3.95$, $p = .003$, $d = -0.82$) but not for randomly presented tones ($t(22) = -1.59$, $p = .169$, $d = -0.33$).

Table 1

Results of the 3-way ANOVA (condition x stimulus x electrode) for repeated measures conducted on the mean ERP-amplitudes (time window 111 - 161 ms) at electrode Fz (upper section). The significant interaction between the three factors included was further analyzed by 2-way ANOVAS (stimulus x electrode) conducted separately for the random condition (middle section) and the predictable condition (lower section).

	Effect	**DFn**	**DFd**	**F**	**p**	**p<.05**	**ges**
100 ms	Condition	1	19	0.831	0.373		0.008
	StimulusType	1	19	1.05	0.318		0.002
	Electrode	1	19	0.036	0.852		0.000331
	Condition x StimulusType	1	19	0.051	0.823		7.55e-05
	Condition x Electrode	1	19	0.763	0.393		0.002
	StimulusType x Electrode	1	19	0.797	0.383		0.001
	Condition x StimulusType x Electrode	1	19	7.53	0.013	*	0.01
150 ms	Condition	1	22	0.08	0.78		0.000263
	StimulusType	1	22	0.317	0.579		0.000339
	Electrode	1	22	0.035	0.854		0.000301
	Condition x StimulusType	1	22	0.16	0.693		0.000124
	Condition x Electrode	1	22	1.13	0.299		0.003
	StimulusType x Electrode	1	22	20.8	0.000155	*	0.026
	Condition x StimulusType x Electrode	1	22	0.053	0.819		4.63e-05

Figure X shows EEG waveform averages for five-tone sequences (A-A-A-A-B) presented in a *predictable* (top panel) and *random* contexts (lower panel).

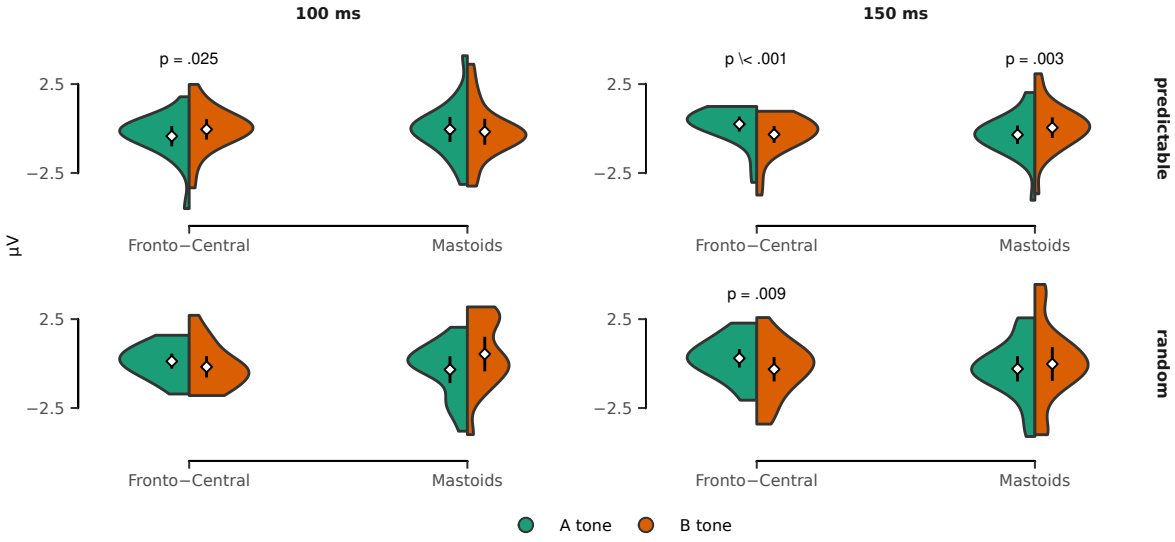

Figure 3. *Averaged voltages in the MMN latency window for pooled fronto-central and mastoid electrodes. Colored areas show sample probability density function for A tones (green) and B tones (red). White diamonds indicate estimated population mean, vertical bars represent 95%-confidence interval. Only Benjamini-Hochberg-corrected p-values* < 0.05 *are shown.*

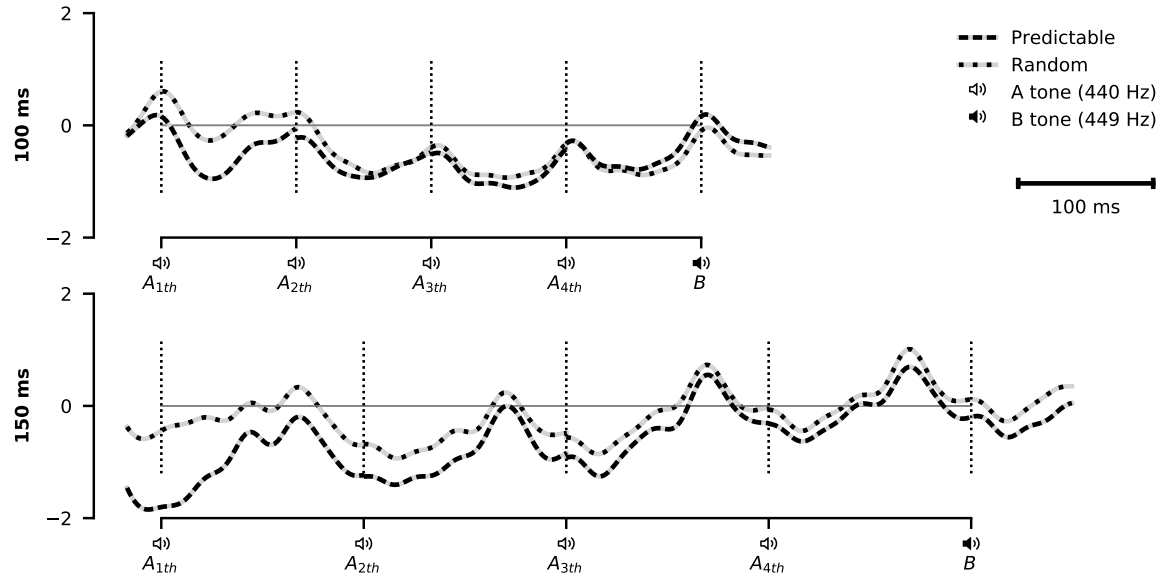

Figure 4. *EEG waveforms for five-tone sequences presented in an predictable context (dotted line) and pseudo-random condition (dashed line) for 100 ms presentation rate (top panel) and 150 ms presentation rate (lower pabel). Vertical lines indicate tone onset.*

Table 2

Results of the 3-way ANOVA (condition x stimulus x electrode) for repeated measures conducted on the mean ERP-amplitudes (time window 111 - 161 ms) at electrode Fz (upper section). The significant interaction between the three factors included was further analyzed by 2-way ANOVAS (stimulus x electrode) conducted separately for the random condition (middle section) and the predictable condition (lower section).

		Effect	DFn	DFd	F	p	p<.05	ges
100 ms	Frontal	Condition	1	19	0.16	.694		0.003
		StimulusType	1	19	0.006	.938		1.5e-05
		Condition x StimulusType	1	19	16.7	\< .001	*	0.013
	Mastoids	Condition	1	19	1.28	.272		0.014
		StimulusType	1	19	1.21	.285		0.004
		Condition x StimulusType	1	19	2.37	.141		0.009
150 ms	Frontal	Condition	1	22	0.947	.341		0.006
		StimulusType	1	22	22.7	\< .001	*	0.038
		Condition x StimulusType	1	22	0.028	.868		2.2e-05
	Mastoids	Condition	1	22	0.206	.655		0.001
		StimulusType	1	22	6.56	.018	*	0.018
		Condition x StimulusType	1	22	0.122	.730		0.00028

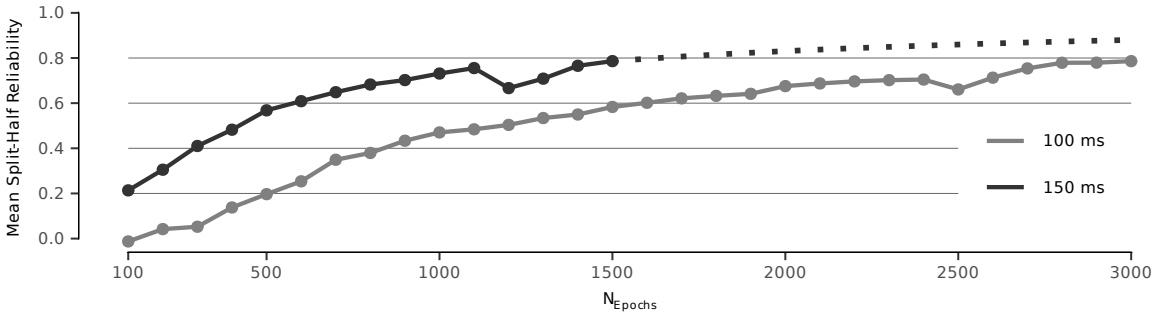

Figure 5. *EEG waveforms for five-tone sequences presented in an predictable context (dotted line) and pseudo-random condition (dashed line) for 100 ms presentation rate (top panel) and 150 ms presentation rate (lower pabel). Vertical lines indicate tone onset.*

References

Ablin, P., Cardoso, J.-F., & Gramfort, A. (2018). Faster independent component analysis by preconditioning with Hessian approximations. *IEEE Transactions on Signal Processing*, *66*(15), 4040–4049. https://doi.org/10.1109/TSP.2018.2844203

Ablin, P., Cardoso, J.-F., & Gramfort, A. (2017). Faster ICA under orthogonal constraint. *arXiv:1711.10873 [Stat]*. http://arxiv.org/abs/1711.10873

Alain, C., Woods, D. L., & Ogawa, K. H. (1994). Brain indices of automatic pattern processing: *NeuroReport*, *6*(1), 140–144. https://doi.org/10.1097/00001756-199412300-00036

Bigdely-Shamlo, N., Mullen, T., Kothe, C., Su, K.-M., & Robbins, K. A. (2015). The PREP pipeline: standardized preprocessing for large-scale EEG analysis. *Frontiers in Neuroinformatics*, *9*. https://doi.org/10.3389/fninf.2015.00016

Brainard, D. H. (1997). The Psychophysics Toolbox. *Spatial Vision*, *10*(4), 433–436. https://doi.org/10.1163/156856897X00357

de Cheveigné, A. (2020). ZapLine: A simple and effective method to remove power line artifacts. *NeuroImage*, *207*, 116356. https://doi.org/10.1016/j.neuroimage.2019.116356

de Cheveigné, A., & Nelken, I. (2019). Filters: When, Why, and How (Not) to Use Them. *Neuron*, *102*(2), 280–293. https://doi.org/10.1016/j.neuron.2019.02.039

Delorme, A., & Makeig, S. (2004). EEGLAB: an open source toolbox for analysis of single-trial EEG dynamics including independent component analysis. *Journal of Neuroscience Methods*, *134*(1), 9–21. https://doi.org/10.1016/j.jneumeth.2003.10.009

Gramfort, A. (2013). MEG and EEG data analysis with MNE-Python. *Frontiers in Neuroscience*, *7*. https://doi.org/10.3389/fnins.2013.00267

Kleiner, M., Brainard, D., Pelli, D., Ingling, A., Murray, R., & Broussard, C. (2007). What's new in psychtoolbox-3. *Perception*, *36*(14), 1–16. https://nyuscholars.nyu.edu/en/publications/whats-new-in-psychtoolbox-3

Mullen, T. R., Kothe, C. A. E., Chi, Y. M., Ojeda, A., Kerth, T., Makeig, S., Jung, T.-P., & Cauwenberghs, G. (2015). Real-time neuroimaging and cognitive monitoring using wearable dry EEG. *IEEE Transactions on Biomedical Engineering*, *62*(11), 2553–2567. https://doi.org/10.1109/TBME.2015.2481482

Nordby, H., Roth, W. T., & Pfefferbaum, A. (1988). Event-Related Potentials to Breaks in Sequences of Alternating Pitches or Interstimulus Intervals. *Psychophysiology*, *25*(3), 262–268. https://doi.org/10.1111/j.1469-8986.1988.tb01239.x

Oldfield, R. C. (1971). The assessment and analysis of handedness: the Edinburgh inventory. *Neuropsychologia*, *9*(1), 97–113. https://doi.org/10.1016/0028-3932(71)90067-4

Perrin, F., Pernier, J., Bertrand, O., & Echallier, J. F. (1989). Spherical splines for scalp potential and current density mapping. *Electroencephalography and Clinical Neurophysiology*, *72*(2), 184–187. https://doi.org/10.1016/0013-4694(89)90180-6

Pion-Tonachini, L., Kreutz-Delgado, K., & Makeig, S. (2019). ICLabel: An automated electroencephalographic independent component classifier, dataset, and website. *NeuroImage*, *198*, 181–197. https://doi.org/10.1016/j.neuroimage.2019.05.026

Saarinen, J., Paavilainen, P., Schöger, E., Tervaniemi, M., & Näätänen, R. (1992). Representation of abstract attributes of auditory stimuli in the human brain: *NeuroReport*, *3*(12), 1149–1151. https://doi.org/10.1097/00001756-199212000-00030

Schröger, E., Tervaniemi, M., Wolff, C., & Näätänen, R. N. (1996). Preattentive periodicity detection in auditory patterns as governed by time and intensity information. *Cognitive Brain Research*, *4*(2), 145–148. https://doi.org/10.1016/0926-6410(96)00023-7

Sussman, E., Ritter, W., & Vaughan, H. G. (1998). Predictability of stimulus deviance and the mismatch negativity: *NeuroReport*, *9*(18), 4167–4170. https://doi.org/10.1097/00001756-199812210-00031

Sussman, E. S., & Gumenyuk, V. (2005). Organization of sequential sounds in auditory memory: *NeuroReport*, *16*(13), 1519–1523. https://doi.org/10.1097/01.wnr.0000177002.35193.4c

Widmann, A., Schröger, E., & Maess, B. (2015). Digital filter design for electrophysiological data – a practical approach. *Journal of Neuroscience Methods*, *250*, 34–46. https://doi.org/10.1016/j.jneumeth.2014.08.002

Winkler, I., Debener, S., Müller, K.-R., & Tangermann, M. (2015). On the influence of high-pass filtering on ICA-based artifact reduction in EEG-ERP. *2015 37th Annual International Conference of the IEEE Engineering in Medicine and Biology Society (EMBC)*, 4101–4105. https://doi.org/10.1109/EMBC.2015.7319296